Article

Extracting the Shape and Size of Biomolecules Attached to a Surface as Suspended Discrete Nano-Particles

Dimitra Milioni, Achilleas Tsortos, Marisela Vélez, and Electra Gizeli

Anal. Chem., **Just Accepted Manuscript** • DOI: 10.1021/acs.analchem.7b00206 • Publication Date (Web): 10 Mar 2017

Extracting the Shape and Size of Biomolecules Attached to a Surface as Suspended Discrete Nano-Particles

Dimitra Milioni[1], Achilleas Tsortos[1,*], Marisela Velez[2], and Electra Gizeli[1, 3, *]

[1] Institute of Molecular Biology and Biotechnology, Foundation for Research and Technology-Hellas, Heraklion, Crete, 70013, Greece

[2] Instituto de Catálisis y Petroleoquímica, CSIC, C/Marie Curie 2, 28049 Madrid, Spain

[3] Department of Biology, University of Crete, Heraklion 71110, Greece

KEYWORDS: acoustic biosensor, QCM-D, intrinsic viscosity, DNA conformation, protein conformation, hydrodynamic model

ABSTRACT: The ability to derive information on the conformation of surface attached biomolecules by using simple techniques such as biosensors is currently considered of great importance in the fields of surface science and nanotechnology. Here we present a nano-shape sensitive biosensor where a simple mathematical expression is used to relate acoustic measurements to the geometrical features of a surface-attached biomolecule. The underlying scientific principle is that the acoustic ratio ($\Delta D/\Delta F$) is a measure of the hydrodynamic volume of the attached entity, mathematically expressed by its intrinsic viscosity [η]. A methodology is presented in order to produce surfaces with discretely-bound biomolecules where their native conformation is maintained. Using DNA anchors we attached a spherical protein (streptavidin) and a rod-shaped DNA (47bp) to a QCM device in a suspended way and predicted correctly through acoustic measurements their conformation, i.e. shape and length. The methodology can be widely applied to draw conclusions on the conformation of any biomolecule or nano-entity upon specific binding on the surface of an acoustic wave device.

Surfaces play an important role in analytical chemistry and bio/nano-technology as they are the platform for molecule immobilization. Achieving surface attachment of biomolecules without changing their native structure impacts on their functionality. For example, biosensors rely heavily on the controlled attachment of protein or DNA molecules so that they maintain their native 3-D conformation and subsequently their activity.[1-3] Nanostructures applied to molecular diagnostics also depend on developing strategies that achieve optimum attachment of nucleic or amino acids to the surface in terms of maintaining their binding efficiency.[4] One of the most sought-after aims in biophysics is obtaining information on the shape/conformation of a surface-attached molecule or changes in its structure due to ligand binding, hybridization, etc. Several techniques have been developed and applied to the structural characterization of attached biomolecules, where analysis focuses on the tertiary conformation of the immobilized entity. Optical evanescent waveguide techniques, such as dual polarization interferometry (DPI), ellipsometry and surface plasmon resonance (SPR) have been used extensively for this purpose. [5,6] By modeling the biological film as a homogeneous and isotropic layer, the equivalent thickness can be estimated and this thickness can be correlated to molecular packing, orientation and size.

Studies employing SPR[7,8] or the ultrasensitive localized surface plasmon resonance (LSPR) method[9,10] have been focused on the dynamic monitoring of protein conformational changes and their exploitation for bio-analytical purposes. Protein conformational changes at a surface have also been detected with the help of a cantilever sensor and miniaturized microarrays.[11] Similar applications have been presented through the use of electrochemical devices[12-14] probing structure-switching events of DNA on a solid support. Self-interference microscopy, another optical method that measures the distance of a fluorescent probe from the surface has been used to estimate the orientation / tilt of surface-tethered DNA.[15] A distinct feature of the above techniques is that, while they can sense conformation-switching events, they cannot pro-

vide any structural information per se for the interrogated molecule. Microscopy techniques such as AFM and TSM are the only methods that can give direct information on the shape and/or orientation of surface-attached molecules at the nanometer level.[16] Difficulties though in imaging soft biological molecules attached through a single point rather than being adsorbed on the surface or embedded in a supported lipid membrane, make these methods not appropriate for routine testing and real time monitoring.

The potential of acoustic devices, such as the Quartz Crystal Microbalance (QCM) and Surface Acoustic Wave (SAW), has been long tested in conformational studies. Such examples include DNA hybridization,[17] the detection of changes in calmodulin during ion or peptide binding,[18,19] in estrogen receptor during DNA binding,[20] in HIV-1 glycoproteins during the binding of small ligands[21] and in aptamers during the binding of ATP,[22] AMP[23] and low Mw analytes.[24] A common approach in the above works is that information is derived from acoustic energy and frequency measurements either qualitatively[18,19,21] or in some cases quantitatively[17,20,22-24] using Voigt-type and other viscoelastic models.[25-27] These models treat the biological layer as a uniform isotropic film and derive information related to the biofilm mass, thickness and rigidity. Some aspects of the hydrodynamic nature of acoustic sensing have been analyzed with 2-D finite element modeling, which treats the adsorbed particles as individual entities,[26,28] and other approaches[29,30] obtaining information about them and the nature of their contact with the sensor surface. A different methodology[31] has been successful in measuring the diameter of nano-sized spheres.[31,32]

Recent studies carried out in our lab introduced a new approach: from the same acoustic measurements, i.e. wave energy and frequency, we showed that it is possible to derive quantitative information on the conformation of the bound analyte at the molecular level obviating the need for a film-based approach. Experimental data combined with theoretical modeling showed that the acoustic ratio of energy losses per unit mass is a measure of the intrinsic viscosity [η] of the bound molecule, i.e., $\Delta D/\Delta F \sim [\eta]$.[33,34] The correlation between intrinsic viscosity and acoustic ratio is significant since [η] is a hydrodynamic parameter characteristic of the shape and size of a biomolecule,[35] parameters directly relevant to biological questions. Moreover, a plethora of experimental and theoretical data exist allowing the direct correlation of [η] to specific geometrical features of a biomolecule, i.e., the length of a rod-shaped nano-particle; the shape of a sphere; the bending-angle of a Γ-shaped molecule, etc.[35,36]

Recently, we measured the acoustic ratio and intrinsic viscosity of over 20 structurally diverse nucleic acids, which were all single-point attached to a neutravidin-modified surface via a biotin link, and verified experimentally the theoretically suggested relationship[33,34] between acoustic ratio and [η]. For a 35 MHz QCM device we found that[37]

$$\left(\frac{\Delta D}{\Delta F}\right)_{35} \cdot 10^3 = 11.2 + 0.34 \cdot [\eta] \qquad (1)$$

where $\Delta D/\Delta F$ is in (10^{-6}/Hz) and [η] in (ml/g). While the above work verified the model which suggested that the acoustic ratio is a measure of [η], the biophysical and bioanalytical value of this expression has not been shown yet.

The purpose of this work is to establish the above methodology as a generic tool for characterizing biomolecules' conformation at a surface. It is shown that if the native shape (i.e., [η]) of a biomolecule is known and is maintained upon attachment to the device surface, it is possible to predict the expected acoustic ratio via Eq. 1, and *vice versa*, from the acoustic ratio it is possible to derive specific geometrical features of the attached molecule. In the current work, this is shown for both protein and DNA molecules. To our knowledge, this is the first time that a label-free biosensor is used to derive quantitative information on the conformation of an attached biomolecule, such as the shape of a protein or length of a double stranded DNA.

EXPERIMENTAL SECTION

Materials and Methods. A Q-Sence E4 (Biolin Scientific, Sweden) acoustic device was employed for real-time simultaneous measurement of frequency and dissipation changes. Au-coated 5 MHz AT-cut quartz crystals were used. The frequency and dissipation responses were recorded at 35 MHz overtone and are presented in their raw form, i.e. not divided by the harmonic number 7. Prior to the experiments, the QCM crystal chips were cleaned in 2% Hellmanex II (Hellma Analytics, Germany) aqueous solution, followed by water rinse and then plasma cleaning for 3 min in a plasma cleaner (Harrick PDC-002, USA) at a "High" setting. All acoustic experiments involved initially a continuous flow (Ismatec ISM935C, IDEX Health & Science GmbH, Germany) of PBS (tablets from Sigma Aldrich, USA) on the biosensor Au-coated surface at a rate of 50 μl/min until a stable frequency and dissipation signal was obtained as baseline. The same flow rate was used throughout all experiments. All measurements were taken at 25 °C.

Streptavidin (Sigma Aldrich) and neutravidin (Invitrogen-Life Technologies) were dissolved in PBS (pH 7.4) at

a final concentration of 20 and 200 μg/ml, respectively. DNA molecules were produced during hybridization of short single stranded strands (Eurogentec SA or Microchemistry Lab) or during PCR amplification. For more details on DNA sequences and experimental procedures see the Supporting Information.

RESULTS

Characterization of the conformation of a protein attached to the surface through a single point. To use the above methodology, it is important that the biomolecule is attached in a way that allows free oscillation around its single anchor point and has no other contact with the surface and its neighboring biomolecules, i.e., maintains its native 3-D structure and full hydrodynamic interaction with the solvent.[37] Moreover, while Eq. 1 was derived for various nucleic acids, here we used a protein as a model biomolecule and specifically, a spherical one. It is known that the lowest possible value for [η] is 2.5 ml/g obtained for a perfect solid sphere. Spherical, or nearly so, proteins have been measured to have [η]=(3.5±1) ml/g (regardless of size),[35] which translates to an equivalent acoustic ratio through Eq.1 of 0.0124×10^{-6}/Hz. In selecting a protein of the right shape and of interest to the scientific community we turned to streptavidin (SAv), a 60 KDa protein comprising a tetramer. Streptavidin is widely used in biotechnology as a substrate for the subsequent immobilization of biotinylated molecules due to its strong affinity for biotin ($K_A \approx 10^{13}$ M^{-1}) through one of its four biotin binding sites.[38] With dimensions of (5.4 × 5.8 × 4.8) nm,[39] its shape can be approximated by a sphere. Although its [η] is not experimentally known, it can be evaluated very accurately by using its known X-ray structure[40] and a theoretical bead model approximation[41]; this approach gives [η] = 3.619 ml/g.

Initially, experiments were performed where SAv (20 μg/ml) was physisorbed on the plasma-cleaned gold QCM crystal surface and the process was followed in real time (Figure S1). A typical change of 145 Hz in ΔF at saturation is accompanied by a very small change in the dissipation, i.e., ΔD ≈ 0.06×10^{-6}/Hz, in good agreement with previous works.[42] Calculating the resulting ratio from Eq.1 gives a value of ≈ $10^{-4}\times10^{-6}$/Hz, which is well below the expected above mentioned value of 0.0124×10^{-6}/Hz for a spherical protein. This ratio suggests that SAv binds tightly to gold through multiple contact points[42] and, thus, cannot be modeled as a molecule surrounded by water and oscillating freely in buffer. To confirm the above results we imaged the SAv exposed QCM Au-surface using atomic force microscopy (AFM). Our data (Figure 1) confirm that the surface is indeed covered by a uniform layer of small structures that are highly ordered and around 5 nm in width, corresponding to the size expected for the SAv protein. The observation that SAv forms 2-D crystal structures has also been made previously.[43,44] The AFM images also illustrate that the applied protein does not form aggregates on the surface and for this reason could be safely used as a model protein for binding as a discrete entity with the help of an appropriate anchor. It should be noted that SAv apparently retains its functionality upon Au surface attachment since it can still bind biotin.[42]

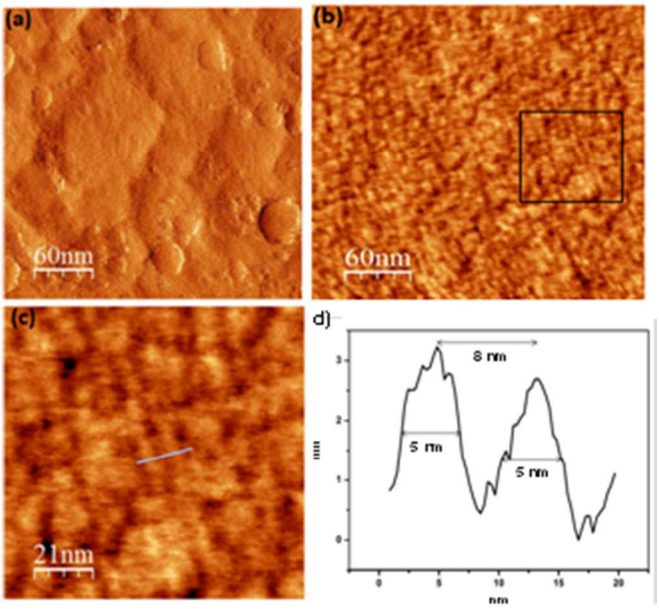

Figure 1. Panel showing phase images of gold surfaces before (a) and after 30 min-incubation (b) with streptavidin and PBS rinsing. Image (a) corresponds to phase image of bare gold and (b) to a monolayer of streptavidin. Image (c) presents the topographic image of the streptavidin monolayer (area under the square in (b)). Panel (d) indicates the height profile under the line in (c), suggesting a typical width of the proteins of 5 nm and distances between them around 8 nm.

In order to achieve SAv binding as discrete particles an experimental methodology was first developed to achieve biomolecule attachment through a single point, producing non-interacting, free-floating / suspended particles. For this purpose, dsDNA was selected as an anchor. DNA is an extremely versatile material which can be produced in various lengths and with easily modifiable functionalized ends.[45] In this work we used double biotinylated DNA molecules, bearing one biotin at the 3′ and another at the 5′ end, aiming at using one of them for surface binding and the other for anchoring SAv to the surface. Figure 2a shows the real time data of the formation of such an interface: surface-adsorbed neutravidin (NAv) (20 μg/ml) is exposed to a double biotinylated 21bp DNA (50 pmol in

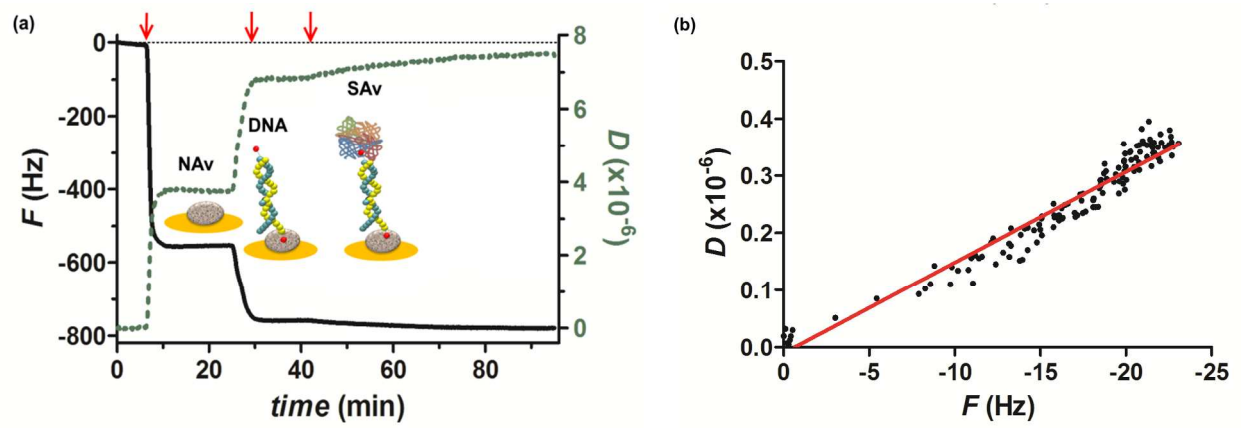

Figure 2. (a) Real time plots of frequency and dissipation during SAv anchoring to a NAv-modified device surface through a double biotinylated 21bp DNA molecule (arrows indicate the time of sample insertion); (b) D versus F plot for SAv binding results in a straight line with a slope of $\Delta D/\Delta F = 0.0152 \times 10^{-6}$/Hz.

200 µL PBS) followed by the addition of SAv (20 µg/ml) which binds to the remaining free biotin-labeled DNA end. Neutravidin, a deglycosylated version of avidin, also with a mass of 60 KDa, was used as the biotin-binding substrate because it was found that SAv does not physisorb on the NAv-coated gold surface (data not shown). From the F and D real time data of SAv binding, a D versus F plot was derived and used to calculate an acoustic ratio of 0.0152×10^{-6}/Hz (Figure 2b). While this ratio is two orders of magnitude larger than the one obtained for SAv on gold, it is also significantly higher to the one predicted by Eq. 1. At first sight this result may appear to question the validity of Eq. 1; however, careful interpretation of the results shows that this is not the case. The correlation between acoustic ratio and [η] reflects energy losses derived from the hydrodynamic interaction of the oscillating molecule in the surrounding liquid. Since SAv is bound to DNA, the observed acoustic ratio should reflect losses due to the oscillation of the DNA/SAv complex and not just the protein. Note that NAv when physisorbed on gold gives a very low acoustic ratio suggesting a very tight binding and is thus considered as an extension of the gold surface.

To separate the contribution of the anchor DNA chain in the acoustic ratio measured for the DNA/SAv complex we systematically changed the length of the DNA. In addition to the 21 bp, DNA molecules of 50 and 76 bp were also constructed; all DNAs had 2 biotins, one at each end and were used for anchoring SAv to the QCM surface (Figure 3a). Real time plots similar to Figure 2a were obtained and used to derive the corresponding acoustic ratios, through D versus F plots, for the other two DNAs (Figure 3b). In parallel, we also studied the possible effect of SAv surface coverage on the acoustic ratio by changing the amount of the DNA added to the surface (DNA concentration range 1-50 pmol). The calculated $\Delta D/\Delta F$ for SAv as a function of SAv load (ΔF_{SAv}) is shown in Figure 3c. According to this figure, the acoustic ratio is independent of SAv surface coverage for all DNA anchor lengths; this suggests that SAv molecules are bound quite apart from each other, preventing potential SAv/SAv cross talk that could affect molecular conformation. While the dependency of acoustic ratio on surface coverage has been reported before[31,46] and also observed in our lab under certain conditions,[47] the specific surface architecture used here prevents this from happening. NAv provides a minimum lateral separation of ≈ 6-7 nm (including the hydration layer) for the attachment of the biotinylated molecules;[33] in addition, only a fraction of the bound DNA is available for subsequent SAv binding, since some DNA molecules may bind through both biotins. The low frequency shifts (max ΔF_{SAv}=40 Hz) obtained during protein attachment in this way is an indication of the limited number of DNA anchors available for subsequent binding (ΔF_{SAv} on Au ≈ 145Hz, Figure S1). It should be noted that larger double biotinylated DNAs (i.e., of >76 bps) failed completely to anchor SAv, probably due to all DNAs binding via both biotins. The observation that the acoustic ratio is independent of surface coverage has been shown before during DNA binding[33,34] and is also true for all DNAs used here.

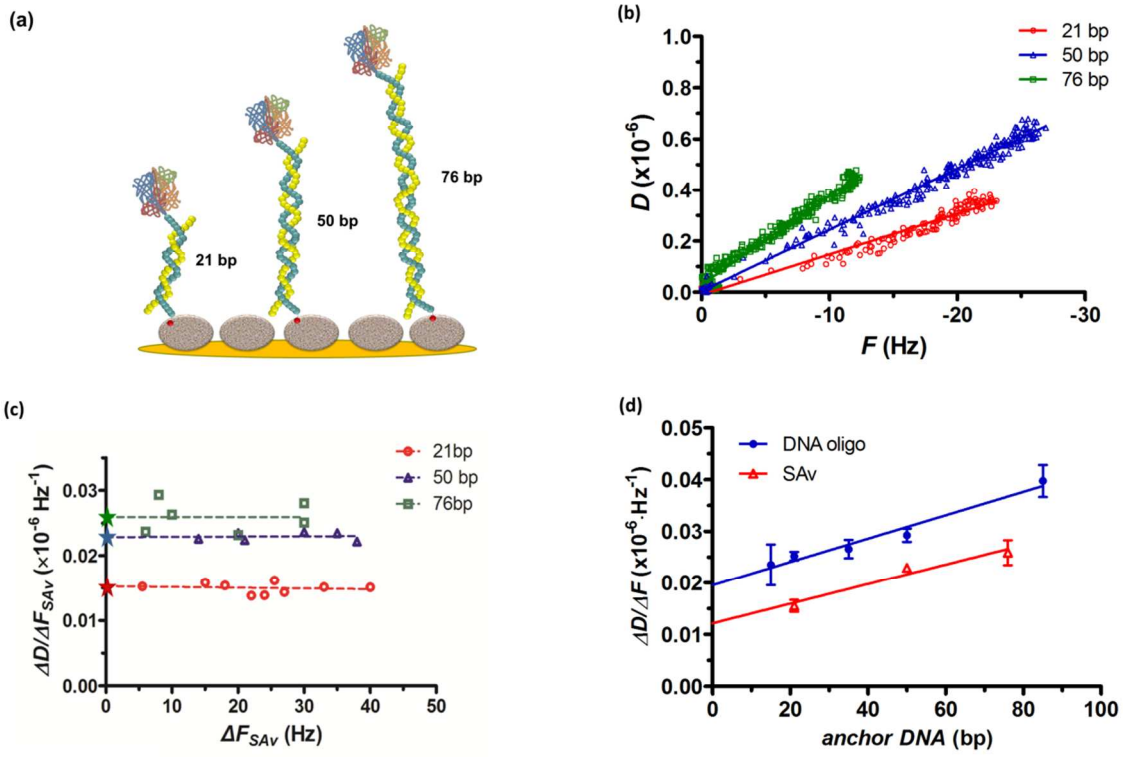

Figure 3. (a) Schematic representation of the 21, 50 and 76bp DNA anchors used to achieve SAv binding through a single point on a NAv-modified Au surface; (b) typical D versus F plots of SAv (20 μg/ml) obtained for each one of the three DNAs; (c) plot of SAv acoustic ratios versus corresponding surface coverage (indicated by ΔF) for each DNA anchor; (d) plot of the acoustic ratio of SAv (red) and 47bp DNA (blue) as a function of the DNA anchor length.

A second observation related to Figure 3c is that the acoustic ratios obtained depend on the number of DNA base pairs, i.e., the length of the anchor chain. This dependency is shown in Figure 3d (red line) where acoustic ratios for SAv are plotted versus the number of base pairs of the DNA anchor. A straight line extrapolation to zero anchor-length leads to a Y-axis intercept corresponding to the ratio of suspended SAv only. This is $(0.0122\pm0.0022)\times10^{-6}$/Hz, i.e., very close to the expected value when using Eq. 1.

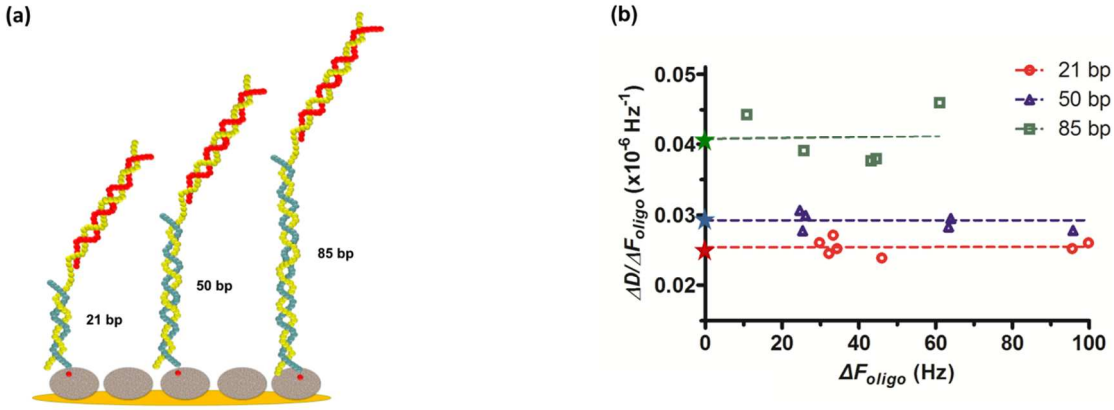

Figure 4. (a) Schematic representation of three DNA anchors (21, 50 and 85bp - lower blue/yellow chain) used to achieve immobilization of the 47nt DNA (upper red chain); (b) plot of the acoustic ratios obtained for the 47 bp DNA as a function of the oligo surface coverage for three DNA-anchors.

Characterization of the 47bp ds DNA attached to the surface through a single point. As verification that the above described approach is more generally applicable, we repeated the same process using a 47 bp DNA chain as the molecule to be suspended; while in our previous works[33,34,37] this molecule was attached to neutravidin via a biotin link, here we sought surface immobilization through DNA anchors. We synthesized dsDNA anchors (see Figure S3), this time of five different lengths (15, 21, 35, 50 and 85 bp) bearing one biotin at their 5′ end and a 47 ds DNA on the other end, the two parts being connected via a flexible three nucleotide hinge (Figure 4a). We again verified the independency of the measured acoustic ratio on surface coverage (Figure 4b) and made the same analysis as with SAv. Plotting the ratio as a function of the number of base pairs of the anchor gives a line which is nearly parallel to the one obtained for SAv (Figure 3d, blue line); the corresponding intercept (0.0195±0.0012)x10-6/Hz, is again in very good agreement with the value (0.0181±0.0020)x10^{-6}/Hz measured during the direct attachment of a biotinylated 50 bp DNA on a NAv modified surface and calculated from Eq. 1.[37,48]

DISCUSSION

The above two examples, in combination with Eq. 1, provide strong evidence of the hydrodynamic nature of acoustic biosensing, at least in the low surface coverage regime and for molecules attached to the surface in a free-floating and suspended way. The use of a molecular model that can be related to known intrinsic physical properties of the attached entity without resort to fitting parameters comes as an alternative to the widely applied optical film-based and acoustic Voigt models. A significant finding of this work is the quantitative and predictive nature of the proposed approach. For the first time it is possible to know in advance what signal to expect from the binding of a nano-entity of a specific shape with a biosensor device. This allows discrimination from the signal between specific and non-specific binding, with the latter always giving a much lower acoustic ratio than that expected for free-floating immobilization. Other obvious advantages are the label-free nature of the method, the requirement for low protein or DNA amounts and the dynamic measurement of conformational changes; the latter was clearly illustrated in previous publications using a Holliday Junction DNA nanoswitch,[49] a DNA nanopump[50] and an intrinsically disordered protein.[47] One of the limitations of the method is of course the need for a molecular anchor in order to immobilize the biomolecule in a suspended / free-floating way. In this study, DNA anchors coupled with a biotin functional group at one end and another biotin or oligonucleotide group at the other were used successfully for streptavidin and nucleic acid attachment. DNA-conjugated antibodies and proteins recently reported in literature[51,52] appear as promising candidates for the general applicability of nucleic acids as molecular anchors. Regarding the resolution of the method, we give the following example; suspension of an IgG molecule (a tri-lobe protein) should be clearly distinguished from the spherical case since $[\eta]_{IgG}$ = (9±1) ml/g,[53] giving an expected acoustic ratio ΔD/ΔF = (0.0143±0.0003)x10^{-6}/Hz well within the resolution of 10% of the acoustic method. For dsDNAs, this resolution corresponds to 10 bp in the range of 20-100 bp.[37]

CONCLUSION

We have shown that acoustic measurements combined with a newly described molecular approach can be used to confirm and even obtain the shape and size of an attached biomolecule, if the latter is suspended on a device surface via a single point. We achieved ligand suspension by using DNA anchors, produced with specific end-functionalities. The fully quantitative nature of the method is described by a single equation, which can predict the acoustic signal if the shape, and hence intrinsic viscosity of a biomolecule, is known. The potential of the method in molecular diagnostics has already been shown during the direct probing of DNA conformation.[54-56] The generic nature and simplicity of this methodology is expected to make acoustic wave devices an even more powerful tool for molecular biophysics and especially nanobiotechnology, where great efforts are currently directed towards confirming or determining the shape of synthetic or natural nano-particles.

ASSOCIATED CONTENT

Supporting Information. AFM measurements, DNA sequences and manipulation (DNA anchor-sequences for streptavidin immobilization, DNA anchor-sequences for the 47bp DNA immobilization, DNA hybridization and amplification), Acoustic measurements (SAv on Au, SAv on DNA, detection of 47bp DNA).

AUTHOR INFORMATION

Corresponding Authors * emails: gizeli@imbb.forth.gr and atsortos@imbb.forth.gr

Author Contributions DM carried out all acoustic experiments and subsequent data analysis and assisted in AFM imaging and manuscript writing; AT was responsible for modeling, data analysis and manuscript writing; MV

was responsible for obtaining AFM images and analyzing them; EG wrote the manuscript and supervised the whole work. All authors have given approval to the final version of the manuscript.

ACKNOWLEDGEMENT

EG acknowledges the financial support of EC through FP7-ICT LOVE-FOOD project (Grant No: 317742) and GSRT/ Ministry of Education, Greece and European Regional Development Fund (Sector Operational Program: Competitiveness and Entrepreneurship, NSRF 2007-2013)/EC (KRIPIS-BIOSYS MIS-448301); AT acknowledges EC through Regpot InnovCrete project (Grant No: 316223). We thank Dr. K. Petratos for providing the X-ray structure of the tetrameric SAv.

ABBREVIATIONS

DNA: Deoxyribonucleic acid, NAv: Neutravidin, SAv: Streptavidin, QCM-D: Quartz Crystal Microbalance with Dissipation Monitoring, AFM: Atomic Force Microscopy

REFERENCES

(1) Sassolas, A.; Leca-Bouvier, B. D.; Blum, L. J. *Chemical reviews* **2008**, *108*, 109-139.
(2) Lee, H. J.; Wark, A. W.; Corn, R. M. *The Analyst* **2008**, *133*, 975-983.
(3) Ahmed, M. U.; Saaem, I.; Wu, P. C.; Brown, A. S. *Critical reviews in biotechnology* **2014**, *34*, 180-196.
(4) Kurkina, T.; Balasubramanian, K. *Cellular and molecular life sciences : CMLS* **2012**, *69*, 373-388.
(5) Escorihuela, J.; Gonzalez-Martinez, M. A.; Lopez-Paz, J. L.; Puchades, R.; Maquieira, A.; Gimenez-Romero, D. *Chemical reviews* **2015**, *115*, 265-294.
(6) Coffey, P. D.; Swann, M. J.; Waigh, T. A.; Mu, Q. S.; Lu, J. R. *Rsc Adv* **2013**, *3*, 3316-3324.
(7) Sota, H.; Hasegawa, Y.; Iwakura, M. *Anal Chem* **1998**, *70*, 2019-2024.
(8) Gestwicki, J. E.; Hsieh, H. V.; Pitner, J. B. *Anal Chem* **2001**, *73*, 5732-5737.
(9) Hall, W. P.; Anker, J. N.; Lin, Y.; Modica, J.; Mrksich, M.; Van Duyne, R. P. *J Am Chem Soc* **2008**, *130*, 5836-5837.
(10) Hall, W. P.; Modica, J.; Anker, J.; Lin, Y.; Mrksich, M.; Van Duyne, R. P. *Nano letters* **2011**, *11*, 1098-1105.
(11) Mukhopadhyay, R.; Sumbayev, V. V.; Lorentzen, M.; Kjems, J.; Andreasen, P. A.; Besenbacher, F. *Nano letters* **2005**, *5*, 2385-2388.
(12) Lubin, A. A.; Plaxco, K. W. *Accounts of chemical research* **2010**, *43*, 496-505.
(13) Plaxco, K. W.; Soh, H. T. *Trends in biotechnology* **2011**, *29*, 1-5.
(14) Idili, A.; Plaxco, K. W.; Vallee-Belisle, A.; Ricci, F. *Acs Nano* **2013**, *7*, 10863-10869.
(15) Moiseev, L.; Unlu, M. S.; Swan, A. K.; Goldberg, B. B.; Cantor, C. R. *Proceedings of the National Academy of Sciences of the United States of America* **2006**, *103*, 2623-2628.
(16) Trajkovic, S.; Zhang, X.; Daunert, S.; Cai, Y. *Langmuir* **2011**, *27*, 10793-10799.
(17) Larsson, C.; Rodahl, M.; Hook, F. *Anal Chem* **2003**, *75*, 5080-5087.
(18) Furusawa, H.; Komatsu, M.; Okahata, Y. *Anal Chem* **2009**, *81*, 1841-1847.
(19) Wang, X.; Ellis, J. S.; Lyle, E. L.; Sundaram, P.; Thompson, M. *Mol Biosyst* **2006**, *2*, 184-192.
(20) Peh, W. Y.; Reimhult, E.; Teh, H. F.; Thomsen, J. S.; Su, X. *Biophysical journal* **2007**, *92*, 4415-4423.
(21) Lee, H. S.; Contarino, M.; Umashankara, M.; Schon, A.; Freire, E.; Smith, A. B., 3rd; Chaiken, I. M.; Penn, L. S. *Anal Bioanal Chem* **2010**, *396*, 1143-1152.
(22) Ozalp, V. C. *The Analyst* **2011**, *136*, 5046-5050.
(23) Serrano-Santos, M. B.; Llobet, E.; Ozalp, V. C.; Schafer, T. *Chemical communications* **2012**, *48*, 10087-10089.
(24) Osypova, A.; Thakar, D.; Dejeu, J.; Bonnet, H.; Van der Heyden, A.; Dubacheva, G. V.; Richter, R. P.; Defrancq, E.; Spinelli, N.; Coche-Guerente, L.; Labbe, P. *Anal Chem* **2015**.
(25) Voinova, M. V.; Rodahl, M.; Jonson, M.; Kasemo, B. *Phys Scripta* **1999**, *59*, 391-396.
(26) Reviakine, I.; Johannsmann, D.; Richter, R. P. *Anal Chem* **2011**, *83*, 8838-8848.
(27) Johannsmann, D. *Macromol. Chem. Phys.* **1999**, *200*, 501-516.
(28) Johannsmann, D.; Reviakine, I.; Richter, R. P. *Anal Chem* **2009**, *81*, 8167-8176.
(29) Ellis, J. S.; Thompson, M. *Phys. Chem. Chem. Phys.* **2004**, *6*, 4928-4938.
(30) Ellis, J. S.; Thompson, M. *Chem. Sci.* **2011**, *2*, 237-255.
(31) Tellechea, E.; Johannsmann, D.; Steinmetz, N. F.; Richter, R. P.; Reviakine, I. *Langmuir* **2009**, *25*, 5177-5184.
(32) Olsson, A. L. J.; Quevedo, I. R.; He, D. Q.; Basnet, M.; Tufenkji, N. *Acs Nano* **2013**, *7*, 7833-7843.
(33) Tsortos, A.; Papadakis, G.; Mitsakakis, K.; Melzak, K. A.; Gizeli, E. *Biophysical journal* **2008**, *94*, 2706-2715.
(34) Tsortos, A.; Papadakis, G.; Gizeli, E. *Biosens Bioelectron* **2008**, *24*, 836-841.
(35) Harding, S. E. *Progress in biophysics and molecular biology* **1997**, *68*, 207-262.
(36) Garcia de la Torre, J.; Bloomfield, V. A. *Biopolymers* **1978**, *17*, 1605-1627.
(37) Tsortos, A.; Papadakis, G.; Gizeli, E. *Analytical Chemistry* **2016**, *88*, 6472-6478.
(38) Green, N. M. *Advances in protein chemistry* **1975**, *29*, 85-133.
(39) Hendrickson, W. A.; Pahler, A.; Smith, J. L.; Satow, Y.; Merritt, E. A.; Phizackerley, R. P. *Proceedings of the National Academy of Sciences of the United States of America* **1989**, *86*, 2190-2194.
(40) Katz, B. A. *J Mol Biol* **1997**, *274*, 776-800.
(41) Ortega, A.; Amoros, D.; Garcia de la Torre, J. G. *Biophysical journal* **2011**, *101*, 892-898.
(42) Wolny, P. M.; Spatz, J. P.; Richter, R. P. *Langmuir* **2010**, *26*, 1029-1034.
(43) Scheuring, S.; Muller, D. J.; Ringler, P.; Heymann, J. B.; Engel, A. *J Microsc* **1999**, *193*, 28-35.
(44) Ebersole, R. C.; Miller, J. A.; Moran, J. R.; Ward, M. D. *J. Am. Chem. Soc.* **1990**, *112*, 3239-3241.
(45) Jones, M. R.; Seeman, N. C.; Mirkin, C. A. *Science* **2015**, *347*, 1260901.
(46) Ray, S.; Steven, R. T.; Green, F. M.; Hook, F.; Taskinen, B.; Hytonen, V. P.; Shard, A. G. *Langmuir* **2015**, *31*, 1921-1930.
(47) Mateos-Gil, P.; Tsortos, A.; Velez, M.; Gizeli, E. *Chem Commun* **2016**, *52*, 6541-6544.
(48) Tsortos, A.; Papadakis, G.; Gizeli, E. *Biopolymers* **2011**, *95*, 824-832.
(49) Papadakis, G.; Tsortos, A.; Gizeli, E. *Nano letters* **2010**, *10*, 5093-5097.
(50) Zhu, D.; Pei, H.; Yao, G.; Wang, L.; Su, S.; Chao, J.; Wang, L.; Aldalbahi, A.; Song, S.; Shi, J.; Hu, J.; Fan, C.; Zuo, X. *Advanced Materials* **2016**, *28*, 6860-6865.
(51) Kazane, S. A.; Sok, D.; Cho, E. H.; Uson, M. L.; Kuhn, P.; Schultz, P. G.; Smider, V. V. *Proceedings of the National Academy of Sciences of the United States of America* **2012**, *109*, 3731-3736.
(52) Mahshid, S. S.; Camire, S.; Ricci, F.; Vallee-Belisle, A. *J. Am. Chem. Soc.* **2015**, *137*, 15596-15599.
(53) Monkos, K.; Turczynski, B. *Int J Biol Macromol* **1999**, *26*, 155-159.
(54) Papadakis, G.; Tsortos, A.; Kordas, A.; Tiniakou, I.; Morou, E.; Vontas, J.; Kardassis, D.; Gizeli, E. *Sci Rep-Uk* **2013**, *3*.
(55) Tsortos, A.; Grammoustianou, A.; Lymbouridou, R.; Papadakis, G.; Gizeli, E. *Chemical communications* **2015**, *51*, 11504-11507.

(56) Papadakis, G.; Tsortos, A.; Bender, F.; Ferapontova, E. E.; Gizeli, E. *Anal Chem* **2012**, *84*, 1854-1861.

SYNOPSIS *TOC*